AIP Journal of Applied Physics

Effect of band alignment on photoluminescence and carrier escape from InP surface quantum dots grown by metalorganic chemical vapor deposition on Si

Nripendra N. Halder, Pranab Biswas, Tushar Dhabal Das, Sanat Kr. Das, S. Chattopadhyay, D. Biswas, and P. Banerji

Citation: Journal of Applied Physics **115**, 043101 (2014); doi: 10.1063/1.4862439
View online: http://dx.doi.org/10.1063/1.4862439
View Table of Contents: http://scitation.aip.org/content/aip/journal/jap/115/4?ver=pdfcov
Published by the AIP Publishing

Effect of band alignment on photoluminescence and carrier escape from InP surface quantum dots grown by metalorganic chemical vapor deposition on Si

Nripendra N. Halder,[1] Pranab Biswas,[2] Tushar Dhabal Das,[3] Sanat Kr. Das,[3] S. Chattopadhyay,[3] D. Biswas,[4] and P. Banerji[2,a)]
[1]*Advanced Technology Development Centre, Indian Institute of Technology, Kharagpur 721 302, India*
[2]*Materials Science Centre, Indian Institute of Technology, Kharagpur 721 302, India*
[3]*Department of Electronic Science, University of Calcutta, 92 Acharya Prafulla Chandra Road, Kolkata 700 009, India*
[4]*Department of Electronics and Electrical Communication Engineering, Indian Institute of Technology, Kharagpur 721 302, India*

(Received 12 September 2013; accepted 2 January 2014; published online 22 January 2014)

A detailed analysis of photoluminescence (PL) from InP quantum dots (QDs) grown on Si has been carried out to understand the effect of substrate/host material in the luminescence and carrier escape process from the surface quantum dots. Such studies are required for the development of monolithically integrated next generation III-V QD based optoelectronics with fully developed Si microelectronics. The samples were grown by atmospheric pressure metalorganic chemical vapor deposition technique, and the PL measurements were made in the temperature range 10–80 K. The distribution of the dot diameter as well as the dot height has been investigated from atomic force microscopy. The origin of the photoluminescence has been explained theoretically. The band alignment of InP/Si heterostructure has been determined, and it is found be type II in nature. The positions of the conduction band minimum of Si and the 1st excited state in the conduction band of InP QDs have been estimated to understand the carrier escape phenomenon. A blue shift with a temperature co-efficient of 0.19 meV/K of the PL emission peak has been found as a result of competitive effect of different physical processes like quantum confinement, strain, and surface states. The corresponding effect of blue shift by quantum confinement and strain as well as the red shift by the surface states in the PL peaks has been studied. The origin of the luminescence in this heterojunction is found to be due to the recombination of free excitons, bound excitons, and a transition from the 1st electron excited state in the conduction band (e_1) to the heavy hole band (hh_1). Monotonic decrease in the PL intensity due to increase of thermally escaped carriers with temperature has been observed. The change in barrier height by the photogenerated electric-field enhanced the capture of the carriers by the surface states rather than their accumulation in the QD excited state. From an analysis of the dependence of the PL intensity, peak position, and line width with temperature and excitation source, the existence of free and bound excitonic recombination together with $e_1 \rightarrow hh_1$ transitions in the QDs is established.
[http://dx.doi.org/10.1063/1.4862439]

I. INTRODUCTION

The low cost and fully developed process technology makes Si the backbone for microelectronic industry. However, due to its indirect band gap it cannot be used for optoelectronic sources.[1] Researchers, thus, worked a lot to get efficient luminescence using porous silicon (PSi)[2,3] and Si nano-crystals[4,5] embedded in SiO_2. However, PSi could not be introduced in the silicon based optoelectronic industry due to the formation of unstable bonds between hydrogen and Si. Furthermore, instability of porous silicon at higher temperature and corrosive ambient prohibit its application.[2] On the other hand, Si nano-crystals embedded in SiO_2 can emit light in the infrared region when their sizes lowered down to 2 nm or less.[4] It has been found in the literature that Si quantum dots having diameter less than 5 nm may have significant luminescence properties due to higher recombination rate and overlapping of electron hole wave functions. However, the quantum yield of the quantum dots (QDs) is very low and needs very careful passivation.[5] On the other hand, III-V semiconductors can be used very efficiently in optical sources due to their tunable and direct band gap. Thus the growth of III-V semiconductors on Si substrates has been found to be of potential interest in the field of monolithic integration of optoelectronics with Si microelectronics. Layer by layer growth of III-V semiconductors on Si is technologically unsuitable due to large lattice mismatch and difference in thermal expansion coefficient between Si and III-V. Such kind of growth introduces large number of threading dislocation leading to non-radiative recombination.[1] Thus one can think for the pseudomorphic layer; then, its thickness within one nanometer is unrealistic in device applications. The growth of polar III-V semiconductors on Si

a)Author to whom correspondence should be addressed. Electronic mail: pallab@matsc.iitkgp.ernet.in

introduces anti-phase domain as well. However, creation of the III-V nanostructures such as quantum dots on Si is advantageous compared to other lattice mismatched conventional III-V structures since strong localization of carriers in the active medium by quantum confinement may led to strong luminescence. Additionally density of states in the low dimensional structures modifies the gain medium to have low threshold voltage during lasing.[6] With the progress of different growth techniques, the growth of InP QDs on Si has become an interesting area of research for different groups.[7,8] It may be mentioned here that apart from the near infrared band gap emission around 925 nm, InP can be used in THz emitters and detectors.[7] As the band gap of the InP QDs can be tuned to emit in the red spectral region, it can be used with the Si based single photon detectors for maximum detection efficiency.[6]

Generally QDs are capped by other high band gap materials for better carrier confinement as the properties of the QDs are dependent on the density and thickness of the cap layer. However, exposed or uncapped QDs will be oxidized, and there will be surface states as well as strain relaxation leading to different interesting phenomenon.[9] The band alignment between the QDs and the host matrix element and the size distribution of the QDs in the ensemble play significant role in the luminescence process. In the literature, some reports on the growth and luminescence of III-V QDs on Si substrate are available.[7,8,10–13] The growths of InAs QDs on Si matrix have been reported by a number of researchers[10–12] with emission around 1.3 μm as obtained from the photoluminescence (PL) study. However, except an attempt by Heitz *et al.*, the emission mechanism is not fully explained.[10] Kumar *et al.*[13] reported the growth of InN QDs on Si and characterized their samples by PL; however, the effect of the size variation on the line broadening has not been discussed. As GaP has the lattice constant very near to Si, some efforts were made to grow InP QDs on GaP as a building block of Si photonics. Growth of InP on GaP substrates and subsequent PL emission has been reported by Guo *et al.*[14] and Masselink *et al.*[15] Though Masselink *et al.*[15] discussed the band alignment of the heterostructure, the effect of particle distribution on the PL line width is not reported.

In the literature it has been found that Ellingson *et al.*[16] reported the charge carrier relaxation in the colloidal InP QDs dispersed in hexane solution. Irradiating with different photon energies, the authors suggested that the relaxation of the charge carriers depends on excitation energy with remarkable reduction in relaxation efficiency. Mićić *et al.*[17] investigated the spectroscopic behavior of InP QDs as a function of their dimension and observed that with the increase in PL excitation power, the line width decreases. It can be mentioned here that all these QDs were prepared through a colloidal route, and the luminescence properties were studied by dispersing them in organic medium. However, since the QDs are normally deposited onto a substrate for device application, any contribution of the substrates will modify the luminescence properties of the QDs. It is observed that various physical phenomena like effect of few particle states, non-linear electron phonon coupling, and non-classical photon statistics have been studied by different groups[18–20] for a well established In(Ga)As QDs grown on GaAs by S-K mechanism. Hessman *et al.*[21] studied the electron accumulation in a single InP QD embedded in InGaP matrix (i.e., both the capping and the base are InGaP) and also reported the global luminescence from the QD ensemble. The authors studied the dependence of PL intensity with applied voltage without mentioning the carrier escape phenomenon or thermal quenching. AbuWaar *et al.*[9] studied the PL of InAs surface QDs grown on GaAs, and the effect of capping layer was discussed elaborately. Though Prunchel *et al.*[7] reported the room temperature photoluminescence while reporting the growth of InP nano-crystals on Si, the details are not found in that work.

In spite of various reports on PL emission from different QDs available in the literature, no study has been made on the temperature dependence of the carrier relaxation with an insight of the band alignment in InP/Si heterostructure. However, without such study the carrier escape mechanism could not be explained. As line broadening originates from different phenomena and it is sample specific, different types of broadening in the luminescence spectra should be studied to understand the emission mechanisms in the materials. A proper investigation is thus necessary for a dot ensemble for better understanding of the physical processes which occur in the nanostructures upon optical irradiation. Thus it has been felt that the PL study of the InP QDs can contribute in understanding various physical phenomena like band alignment of the heterostructure, luminescence process, thermal escape of the electrons, and broadening of the PL peaks. The possibility of Volmer-Weber (V-W) growth of InP QDs[8] on Si may open a horizon in the formation of InP QD based emitter in red spectral region. Thus, in this work, we have studied the optical process in the InP QD ensemble through PL, growing them on Si substrate by means of metalorganic chemical vapor deposition (MOCVD). Theoretical band alignment has been studied. Efforts have also been made to explain the temperature dependent broadening of the PL peaks related to bound and free excitons.

II. EXPERIMENTAL PROCEDURE

InP QDs were grown by a horizontal-type atmospheric pressure MOCVD reactor on p-type (100) c-Si substrates. Trimethylindium (TMIn) and phosphine (PH_3) were used as the precursors for indium and phosphorus, respectively. Hydrogen was used to carry the vaporized metal organic precursors from the bubbler to the reactor. Prior to growth, the substrates were degreased by boiling successively in acetone and methanol for 5 min each. To etch the native SiO_2, the Si substrates were poured in a chemical solution of $HNO_3 + HF + CH_3COOH + H_2O$ for 3 min. Finally all the substrates were rinsed for 6 min in deionised water (18.2 MΩ) and dried using nitrogen gun. All the samples were grown at 560 °C for 15 s to enable V-W growth. The flow rates were kept at 45 sccm for TMIn and 60 sccm for PH_3. The surface morphology of the uncapped dots was characterized by tapping mode Atomic Force Microscopy (AFM) (Agilent Technologies). The absorbance spectroscopy of the QDs samples was performed at room temperature using an

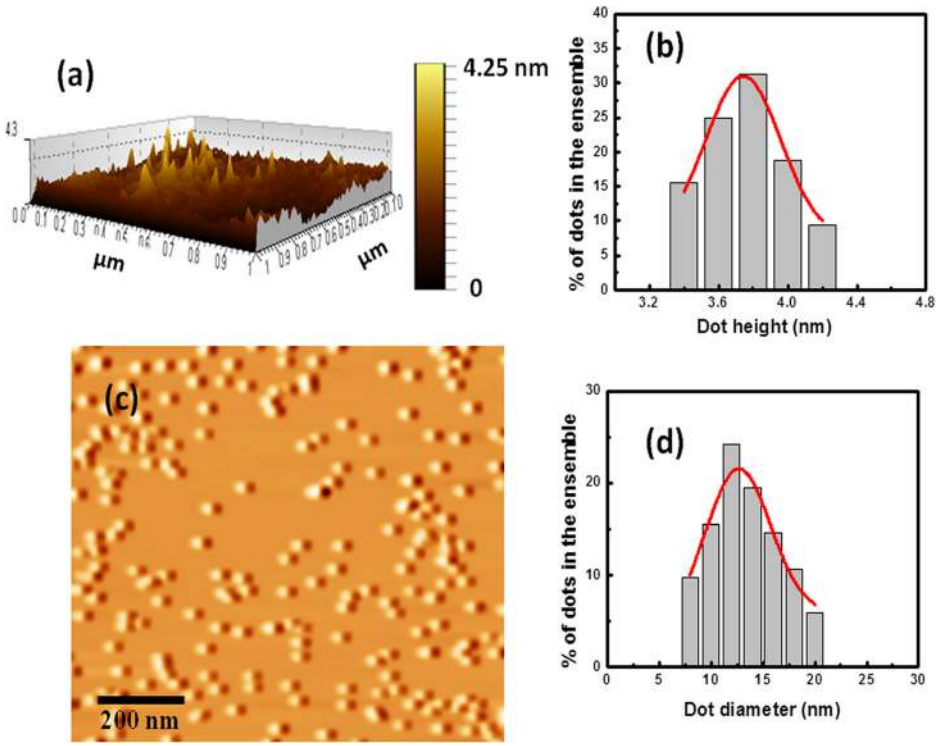

FIG. 1. (a) The surface morphology of the QDs grown on the substrate as viewed by tapping mode atomic force microscopy. The bright spots correspond to the QDs whereas the grey colored region indicates the surface of the substrate. From the grey scale the height of the dots has been found to be within 3.3–4.2 nm. (b) The bar-chart plots the height of the dots as function of their percentage present in the sample. It has a Gaussian distribution with a peak value of 3.74 nm and a variance of ±10%. (c) Two dimensional atomic force micrograph of the quantum dots to estimate their diameters. Migration length related perturbation in the dot diameter has been observed from the diameter variation. The diameter of the dots has a variance from its mean value of 13 nm. (d) Gaussian like distribution in the diameter of the dots.

ultraviolet-visible-near–infrared (UV-VIS-NIR) spectrophotometer (PerkinElmer LAMBDA 750). In order to collect the low temperature PL spectra, the samples were excited with a diode pump solid state laser (RGB Lase, USA) having emission wavelength 532 nm (excitation power 50 mW) mounted in a close cycle liquid He cryostat (APD Cryogenics). The PL system consists of a 0.5 m grating monochromator (Acton Research, USA), a thermocouple cooled InGaAs detector (Acton Research, USA), and a lock-in amplifier (Stanford Research Systems). The PL spectra were taken at five different temperatures from 10 to 80 K. Further increase in temperature could not be possible due to sample heating resulting in excitonic decay.

III. RESULTS AND DISCUSSION

The tapping mode AFM image has been shown in Fig. 1(a). The small bright islands like spots indicate the formation of quantum dots at the grey colored substrate surface. The dot height has been measured, and the percentage of dots having a particular height has been calculated from the processed image. The height of the dots was found to be within 3.3–4.2 nm. In Fig. 1(b), the height distribution of the dots has been plotted. It is observed that the distribution has a peak centered at 3.74 nm, i.e., 30% of the dots having that much height. For other dots, ±0.5 nm (∼10% from the peak value) deviation from the peak is found which suggests controlled growth kinetics has been maintained during the growth. In Fig. 1(c), a variation in the diameter as well as the dot density of the ensemble has been observed from the two dimensional projection of AFM micrograph. The density of dots is determined using WSxM image processing software and has been found to be around $6.2 \times 10^{14}\,m^{-2}$. The bar-chart plot, shown in Fig. 1(d), represents the variation of dot diameter which is found to follow the Gaussian distribution centered at 13 nm. It has been observed that there occurs a variation in the dot diameter due to different migration length of the species on the substrate surface. The fluctuation in the migration length may occur due to the unavoidable atomic level steps such as ledges and kinks present in the substrate. However, the isolated dots on the surface of the substrate confirm the growth mode to be V-W type where no wetting layer is present.

Different excitonic peaks have been observed from the UV-VIS-NIR spectroscopic analysis and have been shown in Fig. 2. The absorbance energy for the ensemble is found to be 1.42 eV (870 nm) which is higher than that of bulk InP (1.34 eV). Higher order transition has also been found at higher energies as the average dimension of the QDs is well below the Bohr exciton radius.

Figure 3 shows the PL spectrum of the sample taken at 10 K. It shows broad luminescence having multiple peaks. As the excitation energy of the laser is much higher than the energy of the QDs, it can be termed as global PL[17] where almost all the dots in the ensemble got excited. The transition of the electrons occurs from the 1st excited state in the conduction band (e_1) to the 1st excited state in the valance band (hh_1) along with different excitonic recombination. A distinct blue shift in the emission spectra has been observed along with different excitonic peaks from the QDs. A notable reduction in the luminescence intensity of some of the peaks has been observed as a signature of different excitons as the excitation power of the laser was decreased. The behavior of the different peaks with the variation of the laser power has been indicated by different regions in Fig. 3. The luminescence presumably coming from the transition $e_1 \rightarrow hh_1$ has been shown by region 1 and found to have not been shifted; however, there is change in intensity. On the other hand the

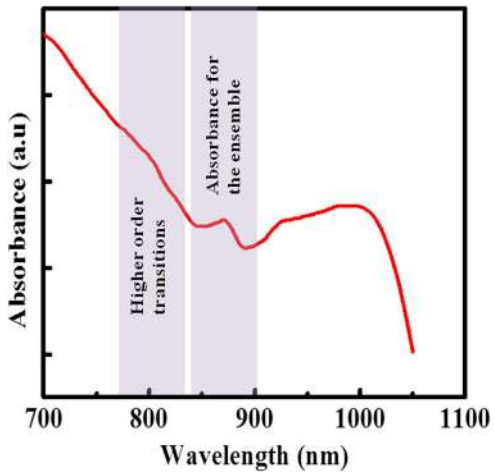

FIG. 2. UV-vis-NIR absorbance spectra of the quantum dot ensemble showing the presence of different transitions.

peaks of region 2 and 3 are coming from excitonic recombination and found to be red shifted with decrease in excitation power. Here it should be mentioned that the higher power of laser will produce local heating in which the excitons will decay. Thus care has been taken to reduce the local heating, and the power of the laser was set at 8 mW, 7 mW and 6 mW for optimum emission output from our previous experience.

As the band lineup between the semiconductors of the heterostructure plays an important role in the luminescence process, let us first discuss the origin of the luminescence from the InP QDs grown on Si substrate with the help of modified model-solid theory[22] and *ab initio* all-electron calculation of absolute volume deformation potentials.[23] These explain the band lineups at the strained interfaces of the semiconductor heterojunctions. Due to 8.1% lattice mismatch between InP and Si, the thickness of the pseudomorphically grown layer will be less than a nanometer. The nanodimensions of the QDs prevent them to be strain relaxed through the formation of dislocations though the thickness of the grown dots is higher than that of their corresponding critical layer thickness. For a typical semiconductor heterostructure system having thickness h_1 and h_2, we can write[24]

$$a_{\parallel} = \frac{a_1 G_1 h_1 + a_2 G_2 h_2}{G_1 h_1 + G_2 h_2}, \tag{1}$$

$$\varepsilon_{i\parallel} = \left[\frac{a_{\parallel}}{a_{\perp}} - 1\right], \tag{2}$$

$$a_{i\perp} = a_i \left[1 - D_i \left(\frac{a_{\parallel}}{a_i} - 1\right)\right], \tag{3}$$

$$\varepsilon_{i\perp} = \left(\frac{a_{i\perp}}{a_{\perp}} - 1\right), \tag{4}$$

where $a_{\parallel}$ and $a_{\perp}$ are the lattice constants parallel and perpendicular to the plane of the interface, ε is the strain, i refers to the corresponding material (1 or 2 respectively), a_i and G_i are lattice constant and shear modulus of the materials under equilibrium circumstances.

The shear modulus can be expressed as

$$G_i = 2\left(c_{11}^i + 2c_{12}^i\right)\left(1 - \frac{D_i}{2}\right), \tag{5}$$

where D is a constant which depends on the elastic constants like c_{11}, c_{12}, etc. of the corresponding material and the interface. In the present case, the thickness of the Si (say, h_1) wafer is much higher than the height of the InP QDs grown on it, i.e., $\frac{h_1}{h_2} \to \infty$, which implies $a_{\parallel} \to a_1$. Thus the grown dots are strained and their dimensions are distorted.

As there is no strain in Si, we can write, $a_{\parallel} = 5.43$ Å. Following Eqs. (1)–(4) one can also get $\varepsilon_{InP\parallel} = -0.075$, $\varepsilon_{InP\perp} = 0.084$, and $a_{InP\perp} = 6.36$ Å.

The modified model-solid theory not only generates the accurate band structure but also helps in aligning the band structure in an absolute energy scale. In this theory the position of the valance band has been calculated initially by means of density functional theory along with the self-consistent pseudopotential technique. The experimentally obtained band gap is added with to get the value of the position of the conduction band. The average position of the valance band $E_{v,\mathrm{av}}$ is considered here to be deformed by a hydrostatic deformation potential caused by the compression of the semiconductor and strain related shift in the electrostatic potential where the absolute volume deformation potential has been obtained according to *ab initio* all-electron calculation. The deformation can be expressed as

$$a_v = \frac{dE_{v,av}}{d\ln\Omega}, \tag{6}$$

where $d\ln\Omega = \frac{d\Omega}{\Omega}$. Here it should be mentioned that the conduction band deformation, a_c, also behaves the same way, and thus the band gap deformation can be written as $a = a_c - a_v$.

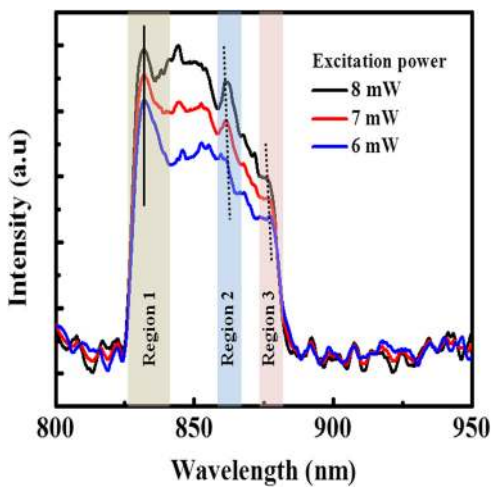

FIG. 3. The global photoluminescence spectra of the quantum dot ensemble acquired at 10 K with different excitation power varied from 8 mW to 6 mW. Multiple peaks in the spectra are the signatures of the height perturbation in the quantum dot ensemble as well as the different types of excitons. The decrease in peak intensity with reduction in laser power in region 1 suggests the recombination of the charge carriers between the 1st excited level in the conduction band (e_1) and heavy hole band (hh_1), i.e., $e_1 \to hh_1$. In both the regions 2 and 3, shift in peak positions and change in their intensity are observed which are due to the presence of different excitons.

For heterojunction, the values of individual band edges are necessary as they have influences in the interface discontinuity. Thus one can write

$$\Delta E_{v,av} = a_v \frac{d\Omega}{\Omega} \tag{7}$$

and

$$\Delta E_{c,av} = a_c \frac{d\Omega}{\Omega}, \tag{8}$$

where $\frac{\Delta\Omega}{\Omega} = (\varepsilon_{xx} + \varepsilon_{yy} + \varepsilon_{zz})$ is the fractional volume change. Due to the spin-orbit interactions the valance band usually splits even in the absence of the shear strain. Hence the edge of the valance band can be estimated as $E_v = E_{v,av} + \frac{\Delta_0}{3}$ and that of the conduction band is given by

$$E_c = E_v + E_g. \tag{9}$$

The parameters needed for the calculation of the band lineups in Si/InP heterojunction has been shown in Table I.

For a large lattice mismatched Si/InP heterojunction, there occurs a strain. As discussed earlier, the strain component in the InP can be estimated using relations (1)–(4), and the volume change can be estimated as $\frac{\Delta\Omega}{\Omega} = -0.065$ which affects the position of $\Delta E_{v,av}$ as well as E_c. Thus $E_{v,av}$ should be modified and can be written as

$$\Delta E_{v,av} = E^0_{v,av} + a_v \frac{\Delta\Omega}{\Omega}. \tag{10}$$

From Eq. (10) and Table I we can write the valance band offset to be 0.03 eV where as the conduction band offset is 0.24 eV.

The band lineup of the heterostructure has been shown in Fig. 4(a). Here it should be mentioned that the presence of a few nm native oxide makes the surface potential lower than the vacuum potential which has been found to be around 5–6 eV.[25] Thus from the theoretical approach the band lineup is found to be type II. The QDs in the present study were not capped by any higher band gap material, and so they can be treated as the surface quantum dots. Thus there will be shift in energy, viz., blue shift due to (i) quantization, and (ii) biaxial strain and (iii) red shift due to surface states or surface roughness. Hence it may be postulated that the resultant shift in the luminescence is a competitive event.

Due to the quantization of the charge carriers in the semiconductor nanostructures, say quantum dots, the electronic energy levels are shifted with respect to those of the bulk. The energy associated with first band to band transition for such QDs can be written as[26]

$$E(R_0) = E_0 + \frac{\hbar^2\pi^2}{2}\left(\frac{1}{m_e} + \frac{1}{m_h}\right)\frac{1}{R^2} - \frac{1.8e^2}{\epsilon}\frac{1}{R^2} + \frac{e^2}{R}\sum_{n=1}^{\infty}\alpha_n\left(\frac{S}{R}\right)^{2n}, \tag{11}$$

where m_e and m_h are the electron and hole effective masses, e is the electronic charge, ϵ is the dielectric constant, α_n is a function of dielectric constant, S is separation between electrons and holes, and R is the radius of the QDs. As the grown dots have difference in height (h) and base (b), R is a function of h and b, and can be expressed as[27]

$$R = \frac{4h^2 + b^2}{8h}. \tag{12}$$

A pictorial representation of R has been shown in Fig. 4(b). All the terms in the right hand side of Eq. (11) corresponds to different types of energy. The first term corresponds to the band gap energy of the bulk, the second term corresponds to the quantum localization energy whereas the third and the fourth term represents the Coulomb potential and polarization energy, respectively.

Hence to understand the effect of particle size on the PL energy *inter alia* the quantized energy, $E(R)$ should be calculated taking calculated taking $m_e = 0.073m_0$, $m_h = 0.6m_0$, and $\epsilon = 12.5$ (Ref. 28) using the following relation:

$$E(R) - E_0 = \frac{5.7364}{R^2} - \frac{0.9971}{R}. \tag{13}$$

For the QDs one can approximately take the polarization term to be one third of the Coulomb potential,[29] and hence we can write

$$E(R) - E_0 = \Delta E_{quantised} = \frac{5.7364}{R^2} - \frac{0.6647}{R}. \tag{14}$$

For our samples there occurred a perturbation in height as well as in base diameter for the grown QDs and the assembly can be treated as an ensemble. Generally such ensemble of self-assembled QDs gives rise to a statistical distribution in the eigenenergies due to quantization.[30] In our case the QDs were excited with energy higher than the emission energies of the individual dots. Several peaks can be observed from the convolution of the peak as a finger print of the perturbation in the QD height. From the height and diameter distribution of the dots, the radius can be estimated as 7.56 nm. As the effective radius is lower than that of Bohr exciton radius, the confinement of carriers is possible in the dots leading to a blue shift in the PL spectra.

TABLE I. Different constants used for the calculation of band lineup in InP/Si nano heterostructure.[22–24]

Semiconductor	Spin-orbit splitting (Δ_0)	Lattice constant (Å)	D^{001}	G^{001}	$E_{v,av}$	a_v	E_g^{dir}	E_c^{dir}	a_c^{dir}	a^{dir}	E_g^{dir}	E_c^{ind}	a_c^{dir}	a^{ind}
Si	0.04	5.43	0.77	3.64	−6.93	2.16	3.37	−3.65	1.98	−0.48	1.17	−5.85	4.18	1.72
InP	0.11	5.87	1.13	1.89	−6.81	1.83	1.42	−5.58	−5.04	−6.31	…	…	…	…

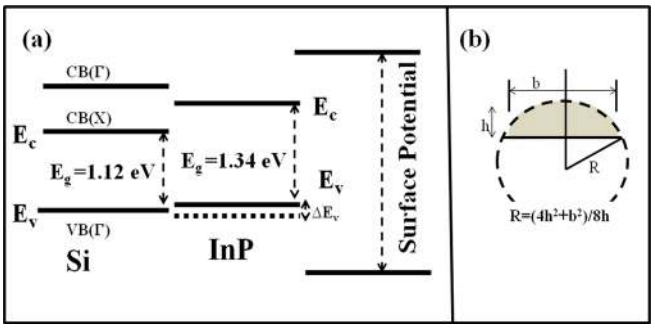

FIG. 4. (a) The band lineup at the InP/Si heterostructure interface. The difference in the valance band has been measured theoretically. The strain related shifts and the splitting have been measured and the details are discussed in the text. (b) Pictorial representation of radius of QDs as a function of height and base.

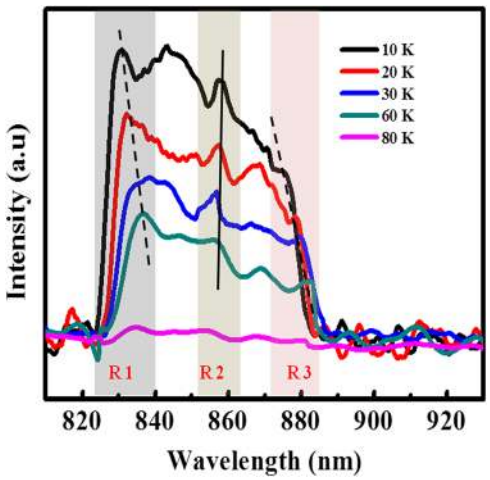

FIG. 5. The photoluminescence spectra of the sample acquired at different temperatures from 10 to 80 K. The decrease in peak intensity with increase in temperature has been detected as the signature of thermo-stimulated quenching process. The peaks corresponding to excited state recombination ($e_1 \rightarrow hh_1$) and bound excitonic recombination is found be red shifted with increase in temperature and has been indicated by the shaded region R1 and region R3, respectively. The peaks marked with solid line in region R2 corresponds to free excitonic peaks and is found to have not shifted with temperature.

On the other hand, a blue shift in the PL peak energy occurs due to the compressive strain produced by Si on the grown InP QDs. The amount of blue shift due to the strain can be estimated by the Pikus-Bir Hamiltonian:[31] $\Delta E_{strain} = 2a\left(1 - \frac{c_{12}}{c_{11}}\right)\varepsilon_{\parallel} - b\left(1 + \frac{2c_{12}}{c_{11}}\right)\varepsilon_{\parallel}$, where a and b are the hydrostatic and shear deformation potential of the semiconductor, respectively. However for the surface quantum dots the presence of the surface states gives rise to the red shift in the PL energy. The energy eigenstates in the QDs are found to be red-shifted when getting in closer proximity to the surface because the absence of the cap allows relaxation in the strain of the QDs.[9] It may be mentioned that such red shift in the energy of the QDs originates from various deep traps and surface states; for smaller dots, the effect is more prominent. It has been observed that the amount of red shift (~90–110 meV) increases with the decrease in the height of the QDs. Thus the total shift can be determined by the competitive effect of the three mechanisms as mentioned above (i)–(iii), and the luminescence peak occurs at an energy which is greater than the bulk band gap energy of InP but less than the energy which could have been obtained due to the quantization. On the other hand as the band lineup is type II by nature, the excited states of the charge carriers lies in different semiconductors and may lead to red shift of the PL spectra.

In Fig. 5, a representative PL spectrum of a sample has been shown. It is observed that the spectrum consists of different narrow peaks originating from transitions from $e_1 \rightarrow hh_1$ and other exciton recombination. However, the recombination process in such QDs may involve longitudinal optical phonons. Generally when a bulk semiconductor is irradiated with a photon flux having energies more than its band gap, the generated electrons and holes share the extra energy so that the total momentum remains constant. As in InP, the heavy hole mass, m^*_{hh}, is 8 times larger than that of the electron effective mass, m^*_e, the electrons should take 8 times more kinetic energy than the holes.[16] However, InP, in spite of being a direct band gap material, the conservation of kinetic energy is necessary but not sufficient due to quantum size effect. Thus, the momentum conservation should also be taken care for which phonon assisted momentum transfer may be useful in understanding the process fully.

It should be mentioned that the host Si substrate was taken p-type with a carrier concentration of $\sim 10^{16}\,cm^{-3}$ and InP has an unintentional n-type doping of $\sim 10^{17}\,cm^{-3}$. Though the doping concentration is low enough, the Fermi level can move to the vicinity of the valance band edge of Si and the conduction band edge of InP at low temperatures and the InP QDs are filled with electrons.[21] Such charging of the dots and the substrate gives rise to a depletion region introducing a band bending at the junction. Thus the optically generated electrons can be captured very easily by hole with a radiative recombination.

From Fig. 5 it is found that the peak intensity of the PL decreases with increase in temperature due to thermo-stimulated quenching. The intensity of the PL is associated with the temperature by the relation $I_{PL}(T) = \frac{I_{PL}(0)}{[1+a\exp(-\frac{\Delta E}{kT})]}$.[30] As the temperature increases from 10 K to 60 K, the PL intensity decreases monotonically and then drastically which is apparent from the intensity value at 80 K. In Fig. 5, three regions of interest in the PL emission spectra are marked for all the temperatures. Those are region 1 (R1) where the peaks are originating due to $e_1 \rightarrow hh_1$ transition, region 2 (R2) where those are due to free excitons and region 3 (R3) for bound excitonic recombination. The Gaussian fittings of R1, R2, and R3 peaks are shown in Figs. 6(a)–6(c), respectively. With decrease in temperature, blue shift is observed for the peaks in R1 and R3 regions whereas peaks shown in R2 have not been shifted.

The fitted curve for the transition between the excited states at different temperatures has been shown in Fig. 6(a) (R1 in Fig. 5) in which the monotonic decrease as well as the broadening of the peaks has been observed. The carrier escape from the QDs to the continuum states of the host matrix increases with the increase in temperature and thereby the intensity of PL emission decreases.[30] As the conduction

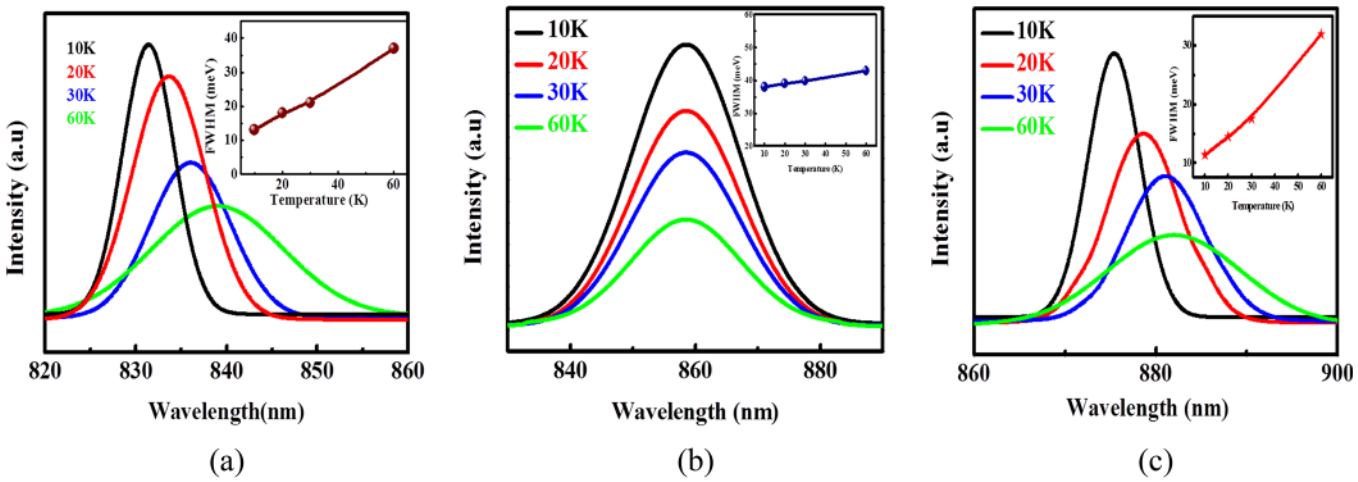

FIG. 6. Gaussian fitting of the peaks related to (a) transition between the excited states (region R1 of Fig. 5), (b) free excitons (R2 of Fig. 5), and (c) bound excitons (R3 of Fig. 5) at different temperatures. The intensity decreases with temperature due to thermo-stimulated quenching process whereas a shift towards higher energy has been detected while the temperature has been decreased. The change in line widths of the respective peaks with temperature has been shown in the insets.

band minima of Si at X-valley is lower than that of the first excited level of InP QDs, the rate of thermal escape increases with temperature due to the change in barrier height by the photo generated electric-field. The thermal expansion of the lattice of the nano-crystals increases with the increase in temperature which alters the wave-function envelope, strain and electron-phonon coupling. The changes of these factors influence the thermal quenching of the PL intensity. The decrease of PL intensity with the temperature also suggests the capture of the carriers by the surface states rather than their accumulation in the QD excited state. Moreover, the modification in the optically allowed and forbidden exciton states can also quench the PL intensity with the increase in temperature. With the quenching of the PL intensity, the PL energy has also been found to be blue shifted with the increase in temperature from 10 K to 60 K. The energy shift for this temperature range has been found to decrease with a temperature co-efficient of $\alpha = (\frac{dE}{dT}) \approx 0.19$ meV/K. At the same time the FWHM is found to be changed with temperature and has been shown in inset of Fig. 6(a). The Gaussian nature of the distribution in the height and diameter of the dots leads to higher order broadening. There will be both homogeneous and inhomogeneous type of broadening with temperature for the excitons related peaks.

The variations of the line width with temperature is shown in insets of Figs. 6(a)–6(c) for three type of transitions discussed above and shown in R1, R2, and R3 regions in Fig. 5. An estimation [from inset of Fig. 6(a)] shows that the rate of change of line width with temperature is 0.5 meV/K whereas in R2 and R3 [Figs. 6(b) and 6(c)] it is 0.014 and 0.4 meV/K. Thus it is observed that the change in line width of the peaks due to free excitonic recombination is almost insignificant compared to that due to bound excitonic recombination. This variation in the linewidth for bound excitonic recombination as well as that due to $e_1 \rightarrow hh_1$ transition followed the temperature dependence of the band gap. Almost similar characteristics of peak shift and line broadening have been obtained while the temperature is increased. These characteristics validate our earlier assumption that the peaks at R3 are coming from bound excitonic recombination having energy lower than the free excitonic recombination energy (R2). The origin of such bound excitons may be either the background impurity present in the dots or the surface states. As the excitation power of the laser used is sufficiently high (8 mW), the excitation may generate more than one electron-hole pair in the dots. In such case the ground state can be occupied by two excitons, and hence there is a possibility of biexciton formation.[32]

In this context it is noteworthy to comment on the different types of broadening occurring in case of PL line width. In semiconductor nano-structures, say QDs, when free excitons are trapped in a state created either by impurity atoms or by any surface state, the states have some finite lifetime with a distribution around a particular value. Furthermore thermal vibration and radiation damping contribute to the homogeneous broadening. Thus the line width of the bound excitonic peaks changes with the change in temperature. On the other hand the inhomogeneous Gaussian broadening occurs due to the Doppler effect arising from the velocity perturbation of the charged particles in the material. The charged particles obey the Maxwell velocity distribution, which, for a particle of mass M and temperature T, can be written as $F(v_x, v_y, v_z) = (\frac{M}{2\pi K_B T})^{\frac{3}{2}} \exp[-\frac{M(v_x^2+v_y^2+v_z^2)}{2K_B T}]$, where $F(v_x, v_y, v_z)dv_x dv_y dv_z$ is the probability of having a particle in the velocity range from v to $v + dv$. Taking the non-relativistic approximation the light emitted in the x-direction with a shifted frequency, $\vartheta - \vartheta_0 = \frac{\vartheta_x \vartheta_0}{c}$, the probability of having the transition frequency between ϑ and $\vartheta + d\vartheta$ can be given by $f(\vartheta)d\vartheta$ which is equal to the probability of finding the same in a range between $\frac{c(\vartheta-\vartheta_0)}{\vartheta_0}$ and $\frac{c(\vartheta+d\vartheta-\vartheta_0)}{\vartheta_0}$ irrespective of values of ϑ_y and ϑ_z. Hence the probability distribution can be written as $f(\vartheta)d\vartheta = \left(\frac{\vartheta}{\vartheta_0}\right)(\frac{M}{2k_B T})^{\frac{1}{2}} \exp[-\frac{(\frac{M}{2k_B T})c^2(\vartheta-\vartheta_0)^2}{\vartheta_0^2}]$. Thus it is found that for an ensemble of QDs, superposition of large number of independent spectral line resulted in a Gaussian profile. Apart from the perturbation of the velocity, the static strain and the surrounding medium also contribute

to the spectral line broadening.[32] The perturbations occurred in the dot ensemble due to variation in dimension and composition of the individual dots leads to the inhomogeneous broadening.[30]

IV. CONCLUSION

Analysis of the PL emission from InP QDs, grown on Si by a horizontal atmospheric pressure MOCVD system, has been made in the present study at different temperatures from 10 to 80 K on varying the power of the excitation laser source to understand the excitonic transitions in an uncapped QD ensemble in a heteroepitaxial system. The emission is found to originate from three different mechanisms, viz., $e_1 \rightarrow hh_1$ transitions, bound and free excitonic recombination. From the variation of the temperature and excitation power source, these transitions were established. The formation of type II heterostructures and the photoluminescence mechanism is discussed through a theoretical study and is examined through physical modeling which includes various individual effects, such as quantization, strain and surface states along with their competitive behavior. The decrease in intensity of the PL emission peaks with temperature is found to be due to carrier escape from the QDs together with thermal quenching. The temperature coefficient of PL emission energy shift corresponding to $e_1 \rightarrow hh_1$ transition is found to be 0.19 meV/K with a line broadening of 0.5 meV/K. The change in line width of the peaks due to free excitonic recombination is almost insignificant compared to that due to bound excitonic recombination. This variation in the linewidth for bound excitonic recombination as well as that due to $e_1 \rightarrow hh_1$ transition followed the temperature dependence of the band gap of the material. Thus in view of the complexity of growth of InP epitaxial layers on Si, QD based structures can be a suitable substitute for future generation heteroepitaxial optoelectronic devices for monolithic integration.

ACKNOWLEDGMENTS

N. N. Halder thankfully acknowledges the financial support received from DST, India (Sanction No. 100/IFD/196/2010-11, dated 03/06/10). The authors are thankful to Mr. P. Chakraborty for his technical help in the growth. AFM measurements were carried out in the Laboratory of Professor Rabibrata Mukherjee (Chemical Engineering Department, IIT, Kharagpur) for which the authors acknowledge his support.

[1]Z. Mi, J. Yang, P. Bhattacharya, G. Qin, and Z. Ma, Proc. IEEE **97**, 1239 (2009).
[2]N. Naderi, M. R. Hashim, J. Rouhi, and H. Mahmodi, Mater. Sci. Semicond. Process. **16**, 542 (2013).
[3]F. Namavar, H. P. Maruska, and N. M. Kalkhoran, Appl. Phys. Lett. **60**, 2514 (1992).
[4]K. S. Cho, N.-M. Park, T.-Y. Kim, K.-H. Kim, G. Y. Sung, and J. H. Shin, Appl. Phys. Lett. **86**, 071909 (2005).
[5]D. Jurbergs, E. Rogojina, L. Mangolini, and U. Kortshagen, Appl. Phys. Lett. **88**, 233116 (2006).
[6]M. Wiesner, M. Bommer, W.-M. Schulz, M. Etter, J. Werner, M. Oehme, J. Schulze, M. Jetter, and P. Michler, Appl. Phys Express **5**, 042001 (2012).
[7]S. Prucnal, S. Zhou, X. Ou, H. Reuther, M. O. Liedke, A. Mücklich, M. Helm, J. Zuk, M. Turek, K. Pyszniak, and W. Skorupa, Nanotechnology **23**, 485204 (2012).
[8]N. N. Halder, S. Kundu, R. Mukherjee, D. Biswas, and P. Banerji, J. Nanopart. Res. **14**, 1279 (2012).
[9]Z. Y. AbuWaar, E. Marega, Jr., M. Mortazavi, and G. J. Salamo, Nanotechnology **19**, 335712 (2008).
[10]R. Heitz, N. N. Ledentsov, D. Bimberg, A. Y. Egorov, M. V. Maximov, V. M. Ustinov, A. E. Zhukov, Z. I. Alferov, G. E. Cirlin, I. P. Soshnikov, N. D. Zakharov, P. Werner, and U. Gösele, Appl. Phys. Lett. **74**, 1701 (1999).
[11]A. Y. Egorov, A. R. Kovsh, V. M. Ustinov, A. E. Zhukov, M. V. Maksimov, G. E. Cirlin, N. N. Ledentsov, D. Bimberg, P. Werner, and Z. I. Alferov, J. Cryst. Growth **201/202**, 1202 (1999).
[12]N. D. Zakharov, P. Werner, U. Gösele, R. Heitz, D. Bimberg, N. N. Ledentsov, V. M. Ustinov, B. V. Volovik, Zh. I. Alferov, N. K. Polyakov, V. N. Petrov, V. A. Egorov, and G. E. Cirlin, Appl. Phys. Lett. **76**, 2677 (2000).
[13]M. Kumar, B. Roul, T. N. Bhat, M. K. Rajpalke, N. Sinha, A. T. Kalghatgi, and S. B. Krupanidhi, J. Nanopart. Res. **13**, 1281 (2011).
[14]W. Guo, A. Bondi, C. Cornet, H. Folliot, A. Létoublon, S. Boyer-Richard, N. Chevalier, M. Gicquel, B. Alsahwa, A. Le Corre, J. Even, O. Durand, and S. Loualiche, Phys. Status Solidi C **6**, 2207 (2009).
[15]W. T. Masselink, F. Hatami, G. Mussler, and L. Schrottke, Mater. Sci. Semicond. Process. **4**, 497 (2001).
[16]R. J. Ellingson, J. L. Blackburn, P. Yu, G. Rumbles, O. I. Mićić, and A. J. Nozik, J. Phys. Chem. B **106**, 7758 (2002).
[17]O. I. Mićić, H. M. Cheong, H. Fu, A. Zunger, J. R. Sprague, A. Mascarenhas, and A. J. Nozik, J. Phys. Chem. B **101**, 4904 (1997).
[18]E. Dekel, D. Gershoni, E. Ehrenfreund, D. Spektor, J. M. Garcia, and P. M. Petroff, Phys. Rev. Lett. **80**, 4991 (1998).
[19]A. Zrenner, M. Markmann, E. Beham, F. Findeis, G. Böhm, and G. Abstreiter, J. Electron. Mater. **28**, 542 (1999).
[20]C. Santori, M. Pelton, G. Solomon, Y. Dale, and Y. Yamamoto, Phys. Rev. Lett. **86**, 1502 (2001).
[21]D. Hessman, J. Persson, M.-E. Pistol, C. Pryor, and L. Samuelson, Phys. Rev. B **64**, 233308 (2001).
[22]A. Qteish and R. J. Needs, Phys. Rev. B **45**, 1317 (1992).
[23]Y.-H. Li, X. G. Gong, and S.-H. Wei, Phys. Rev. B **73**, 245206 (2006).
[24]C. G. Van de Walle, Phys. Rev. B **39**, 1871 (1989).
[25]J. M. Moison, C. Guille, M. Van Rompay, F. Barthe, F. Houzay, and M. Bensoussan, Phys. Rev. B **39**, 1772 (1989).
[26]L. E. Brus, J. Chem. Phys. **80**, 4403 (1984).
[27]O. Gunawan, H. S. Djie, and B. S. Ooi, Phys. Rev. B **71**, 205319 (2005).
[28]M. Razeghi, *The MOCVD Challenge: A Survey of GaIn-AsP-InP and GaInAsP-GaAs for Photonic and Electronic Device Applications* (CRC Press, Boca Raton, 2011).
[29]T. R. Ravindran, A. K. Arora, B. Balamurugan, and B. R. Meheta, Nanostruct. Mater. **11**, 603 (1999).
[30]D. Bimberg, M. Grudmann, and N. N. Ladenstov, *Quantum Dot Heterostructures* (John Wiley & Sons Ltd., England, 1999).
[31]G. L. Bir and G. Pikus, *Symmetry and Strain-Induced Effects in Semiconductors* (Willey, New York, 1974).
[32]D. Dragoman and M. Dragoman, *Optical Characterization of Solids* (Springer, Berlin, 2002).